Nanoscale Imaging of Electronic Surface Transport Probed by Atom Movements Induced by Scanning Tunneling Microscope Current

Yoshiaki Nakamura, Yutaka Mera, and Koji Maeda*

Department of Applied Physics, Graduate School of Engineering, The University of Tokyo, Bunkyo-ku, Tokyo 113-8856, Japan
(Received 18 February 2002; published 12 December 2002)

The hopping movements of Cl atoms on a Si(111)-(7 × 7) surface that are enhanced by an electron injection from tips of a scanning tunneling microscope (STM) exhibit a spatial spread from the electron injection point with an anisotropic distribution. The enhanced hopping effect becomes greatest at a sample bias voltage being resonant with the Si-Cl antibonding states and also exhibits an oscillatory decay with the distance from the injection point characterized by the wavelength depending on the bias voltage. All of these facts can be interpreted in terms of the coherent expansion of the electron wave packets locally formed at the STM tip.

Recent progress in experimental technology, which has enabled us to study the motion of atoms with a spatial resolution of subnanometers or with a time scale down to some femtoseconds, has allowed us more direct access to the dynamical processes of small quantum systems as molecules in chemical reactions. Particularly, the atomic reactions induced by electronic excitations are intensively studied because of not only the technological curiosity but also of the academic concerns on the underlying physics. In solids, the ''molecules'' to react usually have some coupling with the solid medium. The photoillumination, the most common mean of the electronic excitations, could *directly* excite the molecules, but in such a case the coupling with the medium determines the efficiency of the excitation-induced reaction. On the contrary, the optical excitations may be primarily delocalized in the medium as in the interband excitations; in this case, the coupling between the molecule and the medium facilitates the localization of the primary excitation to the molecule for the reaction to be activated [1]. Recently, an increasing amount of evidence has been found concerning the effects of electronic excitations induced by carrier injection from probe tips of the scanning tunneling microscopes (STM) [2–8]. In contrast to the last case in optical excitations, the probe excitation is of scientific interest in two respects: The excitation is initially localized beneath the tip, but in many cases the effect of the carrier injection is found to spread in space from the injection point [5,9].

In one of our earlier studies [9], we found that an electron injection from an STM tip induces the diffusional hopping of chlorine atoms chemisorbed on Si(111)-(7 × 7) surfaces, while exhibiting three experimental features: (i) The hopping rate becomes greatest at a sample bias voltage V_S around +4.0 V, where a chlorine-originated peak is detected in the local density of states (LDOS) spectrum measured by the scanning tunneling spectroscopy. (ii) The chlorine atom hopping rate increases linearly with the tunneling current.

(iii) The effect of the electron injection spreads over distances of 10 nm from the injection point but does not extend beyond surface step edges. Considering that the LDOS peak at $V_S = +4.0$ eV can be identified as a $\sigma^*_{\text{Si-Cl}}$ antibond orbital according to a theoretical calculation by Schlüter and Cohen [10], we proposed that the electrons primarily injected from the STM tip first *coherently* propagate in a two-dimensional surface band until they escape from the surface band or are trapped *resonantly* by the $\sigma_{\text{Si-Cl}}$ antibonding orbital associated with a Cl adatom, leading to the instabilization of the Si-Cl bond and the diffusion of the Cl atom. In this study, we show that the electron injection effect exhibits an anisotropic spread with an oscillatory dependence on the distance from the tip position, which can be interpreted in terms of a coherent wave packet propagation of electrons in a surface resonance band that is observable at room temperature. Hence, the experimental configuration will provide a new scheme to investigate electronic transport in solid surfaces on a nanometer scale.

The samples cut from an arsenic-doped *n*-type Si(111) wafer were degassed, cleaned by the conventional method at a base pressure of $\sim 6 \times 10^{-9}$ Pa to prepare reconstructed (7 × 7) surfaces and then subjected to exposure to a chlorine beam from an AgCl electrolytic cell until 30% of the adatom sites were covered with chlorine atoms. The prepared samples transferred to an ultrahigh vacuum chamber of STM (UNISOKU) were examined with mechanically sharpened Pt-Ir tips outgassed at $\sim 600\,°$C for 10 min under a pressure of $\sim 1 \times 10^{-7}$ Pa. The use of sharp tungsten tips fabricated by using a laboratory-built electrolytic etching apparatus did not change the results. The STM observations were conducted at a sample bias of $V_S = +1.0$ V and a tunneling current of $I_T = 80$ pA, under the condition of which we confirmed that the imaging procedures induce no change of the surface structures.

Figures 1(a) and 1(b) show the STM images of a chlorinated Si(111)-(7 × 7) surface before and after,
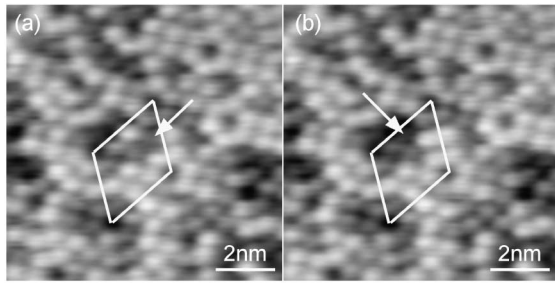
FIG. 1. STM images of a chlorinated Si(111)-(7 × 7) surface before (a) and after (b) electron injection from the probe tip scanned at $V_S = +4.0$ V and $I_T = 80$ pA. The Si adatom sites absorbing chlorine atoms are imaged in dark contrasts. A Cl-adsorbing site indicated with an arrow in (a) has moved to an adjacent site indicated with an arrow in (b), which demonstrates an event of chlorine atom diffusion.

FIG. 2. The contour map of the enhanced jump frequency around the electron injection point at the origin drawn for a crystallographically equivalent sector. (a) The experimental result and (b) the theoretical prediction from Eq. (5) which reproduces quite well the spatial spread significantly anisotropic with respect to the orientation.

respectively, the electron injection from the probe tip scanned at $V_S = +4.0$ V and $I_T = 80$ pA. The Si adatom sites, which would be imaged in light contrasts if the surface is clean, are imaged in dark contrasts when they absorb chlorine atoms on the top [11]. The chlorine atoms were not uniformly distributed on the surface. The dark contrast representing a Cl-adsorbing site indicated with an arrow in Fig. 1(a) is seen to have moved to an adjacent site indicated with an arrow in Fig. 1(b), which demonstrates an event of chlorine atom diffusion. As reported previously, even when we localized the electron injection in an area as small as 1.6 nm × 1.6 nm, the enhanced chlorine jumps were observed also at positions appreciably far from the injection area. We found that the spatial spread is neither uniform nor isotropic. Figure 2(a) shows the event frequency, plotted for a crystallographically equivalent sector [12], of the chlorine jump (averaged for 74 frames) per electron and per chlorine atom in a unit area. The spreading effect predominates in the directions of $\langle \bar{1}\bar{1}2 \rangle$ and $\langle \bar{1}01 \rangle$. The dependence of the enhanced jump rate on the distance from the electron injection point (in this case not scanned) beneath the tip, biased at two different bias voltages, is plotted in Fig. 3 for the two orientations $\langle \bar{1}\bar{1}2 \rangle$ [3(a)] and $\langle \bar{1}01 \rangle$ [3(b)]. The radial event probability $g(r; \phi)$ in the abscissas is defined as the number (averaged for 74 frames) of chlorine jump events per electron and per chlorine atom observed in an infinitely small area $r dr d\phi$ at radial distance r from the tip position and at the orientation angle ϕ. The closed and open circles present results obtained both at $I_T = 80$ pA, but at $V_S = +4.0$ V and $V_S = +4.1$ V, respectively. A fact to be noted is that the $g(r; \phi)$ vs r curves exhibit an oscillatory damping behavior with peaks at different distances, at 6.5 and 14.5 nm for $V_S = +4.0$ V, and at 3.5 and 7.5 nm for $V_S = +4.1$ V in Fig. 3(a); and at 4.5, 7.25, and 13.5 nm for $V_S = +4.0$ V, and at 2.5, 4.5, and 6.5 nm for $V_S = +4.1$ V in Fig. 3(b).

In our previous study [9], we showed that the degree of the spreading effect does not depend on the chlorine coverage, ruling out the model that the surface states
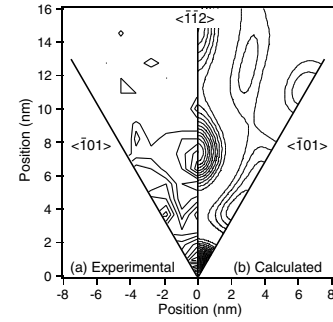
serving the electron propagation originate in the chlorine adsorbates. Instead, we hypothetically attributed the surface band associated to the clean Si(111)-(7 × 7) surfaces. Although previous inverse photoemission spectroscopy (IPES) studies [13,14] attributed the states around the energy of 4 eV above the Fermi level to the bulk states, the blocking of the spreading effect by surface step edges strongly suggests that the states to which the electrons are primarily injected have a large amplitude at the surface. According to the theoretical calculation for the Si(111) ideal surface [10], there is a surface resonance band around 4 eV, originating in the antibonding orbitals of backbonds of the Si adatoms having a dispersion along the Γ to K branch in $\langle \bar{1}01 \rangle$ directions as shown in Figs. 4(a) and 4(c). Although no theoretical calculation on the Si(111)-(7 × 7) surface has been done for this high energy range, the experimental IPES studies of the Si(111) with
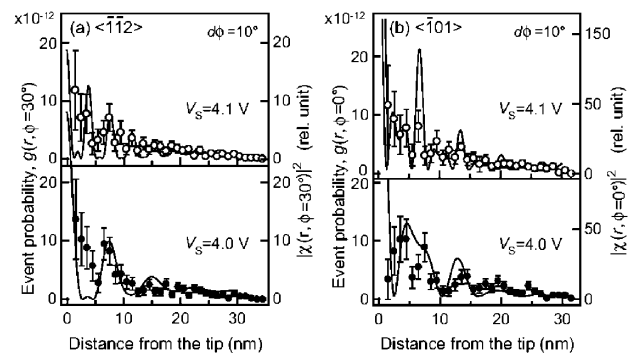
FIG. 3. The radial probability $g(r; \phi)$ of the enhanced chlorine jump, defined as the number of chlorine jump events per electron and per chlorine atom in an infinitely small area, $r dr d\phi$, at radial distance r from the tip position, plotted as a function of the distance r measured along (a) $\langle \bar{1}\bar{1}2 \rangle$ ($\phi = 30°$) and (b) $\langle \bar{1}01 \rangle$ ($\phi = 0°$) orientations within an angular width of $d\phi = 10°$. The closed and open circles present results obtained both at $I_T = 80$ pA , but at $V_S = +4.0$ V and $V_S = 4.1$ V, respectively. The oscillatory decay behaviors are reproduced by theoretical Eq. (5) (see text).
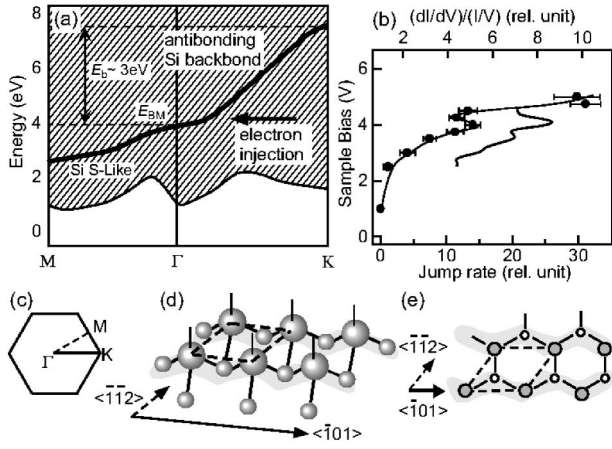
FIG. 4. The surface band (a) calculated by Schlüter and Cohen [10], to which the electrons are to be injected at $V_S = +4$ V [the peak voltage in the sample bias dependence of the chlorine jump rate, see (b)], originates in antibonding backbonds of the Si adatoms with a large dispersion along Γ-K branches in $\langle\bar{1}01\rangle$ directions (c). The bond configuration is illustrated in (d) and its (111) projection in (e). The broken curve in (b) indicates the LDOS at chlorinated sites.

different overlayers [13,14] indicate that the state around 4 eV is insensitive to the surface structure. Therefore, Figs. 4(c) and 4(d) are considered to depict reasonably well the surface resonance band also in Si(111)-(7 × 7) surfaces as far as the band associated with the Si adatom backbonds is concerned. Thus, the anisotropy observed in Fig. 2(a) may be interpreted by the model that the electron propagation occurs along this surface resonance band with a large dispersion along $\langle\bar{1}01\rangle$ directions.

A quantitative account for the anisotropic spreading effect shown in Fig. 2(a) and the oscillatory decay behavior of the $g(r;\phi)$ curves in Fig. 3 is possible in the framework of this model. Generally, for a Hamiltonian explicitly independent of time t, the wave packet function $\psi(\vec{r}, t; t_0)$ of a particle at position $\vec{r}$ evolves with time t from the initial function $\psi(\vec{r}, t_0)$ at time t_0 as

$$\psi(\vec{r}, t; t_0) = \sum_u \int \varphi_u^*(\vec{r}')\psi(\vec{r}', t_0)d\vec{r}' \exp[-iE_u(t - t_0)]$$
$$\times \varphi_u(\vec{r}), \qquad (1)$$

where E_u and $\varphi_u(\vec{r})$ represent the eigenenergies and the eigenfunctions of the Hamiltonian, respectively. Without losing generality, we set $t_0 = 0$. The probability amplitude of the particle having energy E at position $\vec{r}$ is

$$\chi(\vec{r}, E) = \int dt \psi(\vec{r}, t; t_0 = 0) \exp(iEt/\hbar)$$
$$\equiv \int d\vec{r}' G(\vec{r}, \vec{r}', E)\psi(\vec{r}', t_0 = 0). \qquad (2)$$

Here, Green's function $G(\vec{r}, \vec{r}'; E)$ is defined by

$$G(\vec{r}, \vec{r}'; E) = \sum_u \frac{\varphi_u(\vec{r})\varphi_u^*(\vec{r}')}{E - E_u + i\eta}. \qquad (3)$$

The parameter η represents the energy dissipation of the system relevant in the open systems coupled to an environment. In the present situation where the electron is injected locally beneath the tip, the initial function, $\psi(\vec{r}', t_0 = 0)$, is approximated by an s-like (Gaussian) wave function of the tip positioned at the distance z_t above the surface origin ($\vec{r}_{\parallel} = 0$) and, hence, is given for simplicity by a delta function $\delta(|z - z_t|)\delta(|\vec{r}_{\parallel}|)$. The eigenwave functions to be considered are those associated with the surface. Neglecting for a simplified argument the perturbational effects of the STM tip, we write the surface eigenfunctions φ_u as

$$\varphi_u(\vec{r}) = \varphi_{\vec{k}_{\parallel}}(\vec{r}) \sim \exp[-\kappa z]\phi_{\vec{k}_{\parallel}}(\vec{r}_{\parallel})\exp[i\vec{k}_{\parallel} \cdot \vec{r}_{\parallel}], \quad (4)$$

where κ denotes the decay constant determined by the work function, and $\phi_{\vec{k}_{\parallel}}(\vec{r}_{\parallel})\exp(i\vec{k}_{\parallel} \cdot \vec{r}_{\parallel})$ the surface Bloch function with the two-dimensional wave vector $\vec{k}_{\parallel}$ parallel to the surface. The eigenenergies E_u are given by $E_{\vec{k}_{\parallel}} = \hbar^2 k_{\parallel}^2/2m^* + E_{BM}$ (m^*: effective mass of electrons traveling with a wave vector $\vec{k}_{\parallel}$; E_{BM}: band bottom energy). If the jump of a chlorine atom is enhanced with a probability proportional to the density of the electrons at the Cl site with energy E_{σ^*} that is resonant with the Si-Cl antibonding orbital $\sigma^*_{Si\text{-}Cl}$ energy, the radial event probability $g(r;\phi)$ or the event frequency at the arbitrary position is

$$g(r;\phi) \propto |\chi(\vec{r}, E_{\sigma^*})|^2$$
$$\approx \left| \int d\vec{r}' \sum_{\vec{k}_{\parallel}} \frac{\varphi_{\vec{k}_{\parallel}}(\vec{r})\varphi_{\vec{k}_{\parallel}}^*(\vec{r}')}{E_{\sigma^*} - E_{\vec{k}_{\parallel}} + i\eta} \delta(z' - z_t)\delta(|\vec{r}_{\parallel}'|) \right|^2$$
$$\propto \left| \sum_{\vec{k}_{\parallel} = \langle\bar{1}01\rangle} \frac{\exp[i\vec{k}_{\parallel} \cdot \vec{r}]}{E_{\sigma^*} - \hbar^2 k_{\parallel}^2/2m^* + 2\pi i\hbar/\tau} \right|^2. \qquad (5)$$

Here we have introduced electron lifetime $\tau \equiv 2\pi\hbar/\eta$ and assumed that the summation $\sum_{\vec{k}_{\parallel}}$ be taken only for $\vec{k}_{\parallel} = \langle\bar{1}01\rangle$ because, as already noted, the band states into which the electrons are injected are in the Γ to K branches (we assume that the less dispersed band states close to Γ-K branches can be neglected).

The experimental data in Figs. 2 and 3 can be fitted by Eq. (5) with adjustable parameters m^*, $k_{\parallel}$, and τ. If we assume a sinusoidal dispersion, $m^* \approx 2\hbar^2/[E_b(3/4a)^2]$, where a (= 0.384 nm) is the periodicity of the Si backbonds and E_b is the width of the surface band. The value of $k_{\parallel}$ pertinent in Eq. (5) is determined by the energy of the electron injected at the given bias voltage V_S as $k_{\parallel} = \sqrt{2m^*(eV_S - E_{BM})}/\hbar$, where E_{BM} is measured from the sample Fermi level. According to the calculation by Schlüter and Cohen [10], the surface resonance band of the discussed nature, $E_b \approx 3$ eV in width, is located at $E_{BM} \approx 4$ eV. From these values, we could estimate $m^* = 0.61m_e$ (m_e: the electron mass), and if we reasonably assume $E_{BM} = 3.94 \pm 0.02$ eV, $k_{\parallel} = 0.94 \times 10^9$ m^{-1} for $V_S = +4.0$ V, and $k_{\parallel} = 1.79 \times 10^9$ m^{-1} for $V_S = +4.1$ V. The decay with a distance from the tip position is determined by the electron lifetime τ. The contour map

in Fig. 2(b) and the curves in Fig. 3(b) are drawn by using the above parameters and a fitting parameter $\tau = 100$ fs. The anisotropic spreading effect, the periods of the oscillation peaks, and their shift with bias voltage are all well reproduced [15]. It should be noted that the spreading along $\langle \bar{1}\bar{1}2 \rangle$ orientations occurs due to an interference of the electron plane waves propagating in the $\langle \bar{1}01 \rangle$ directions.

The oscillatory behavior of $g(r; \phi)$ can be thus attributed to essentially the same mechanism as the standing waves observed in the derivative conductance (dI/dV) images near step edges on noble metal surfaces [16,17] and around ionized impurities on semiconductor surfaces [18]. The role of the energy window in dI/dV imaging is played by the resonant coupling of electrons to the $\sigma^*_{\text{Si-Cl}}$ state. Although such quantum interference effects are more clearly observed at low temperatures [16,18], conducting experiments at low temperatures is not an essential requirement [14]. The electron lifetime is determined by two factors: the phonon scattering and the resonance of the surface states with the bulk band states. The magnitude of $\tau = 100 \pm 40$ fs for good fits with experiments might be reasonable for the phonon scattering lifetime and the resonance lifetime. The present success in observing quantum interference even at room temperature is mainly owing to the fact that counting atomic events as in the present study yields a higher signal to noise ratio than measuring analog signals such as a tunneling current in the STM.

The weakness of the scattering by the Cl atoms is suggested by the anisotropic spread reflecting the band character of the clean surface and the absence of concentric ripple structures previously observed in dI/dV images around impurities. From ΔE_{σ^*} ($= 0.3$ eV), the experimental FWHM (full width at half maximum) of the $\sigma^*_{\text{Si-Cl}}$ LDOS peak [Fig. 4(b)], the electronic transition time between the $\sigma^*_{\text{Si-Cl}}$ state and the substrate is estimated to be $\Delta t = 2\pi\hbar/\Delta E_{\sigma^*} \approx 14$ fs. Since the mean propagation velocity of the injected electrons along the surface band is $v \approx (1/\hbar)/(\partial E_{\vec{k}_\parallel}/\partial k_\parallel)|_{k_\parallel = 10^{9-10} \, \text{m}^{-1}} \approx 2 \times 10^5$ m/s, the electron traveling distance during the transition time is estimated to be $v\Delta t \approx 3$ nm, which might be long enough for the presence of the Cl atoms to have negligible scattering effects. The conventional straightforward method to investigate electronic transport is the two- or four-probe scheme. In the analogy of the two-probe method, one may view the STM tip as one probe to inject carriers and the Cl atoms as another probe that detects the electron transport to different positions and in different orientations. However, the dimension accessible by the present scheme is much smaller and can be reduced down to a nanometer scale.

In summary, we found that the spread of the electron injection effect on Cl atom diffusion on a Si(111)-(7 × 7) surface exhibits an anisotropic enhancement extending to $\langle \bar{1}\bar{1}2 \rangle$ and $\langle \bar{1}01 \rangle$ crystallographic directions and an oscil-latory decay with the distance from the tip position. These facts are well accounted for by considering the coherent propagation of an electron wave packet along the surface resonance band. Thus, the present type of experiments can provide a new approach to investigate an electronic transport on a nanometer scale.

*Electronic address: maeda@exp.t.u-tokyo.ac.jp

[1] V. May and O. Kühn, *Charge and Energy Transfer Dynamics in Molecular Systems* (Wiley-VCH, Berlin, 2000).

[2] T.-C. Shen, C. Wang, G. C. Abeln, J. R. Tucker, J. W. Lyding, P. Avouris, and R. E. Walkup, Science **268**, 1590 (1995).

[3] G. Lengel, J. Harper, and M. Weimer, Phys. Rev. Lett. **76**, 4725 (1996).

[4] B. C. Stipe, M. A. Rezaei, W. Ho, S. Gao, M. Persson, and B. I. Lundqvist, Phys. Rev. Lett. **78**, 4410 (1997).

[5] B. C. Stipe, M. A. Rezaei, and W. Ho, Phys. Rev. Lett. **79**, 4397 (1997).

[6] E. T. Foley, A. F. Kam, J. W. Lyding, and P. Avouris, Phys. Rev. Lett. **80**, 1336 (1998).

[7] K. Stokbro, C. Thirstrup, M. Sakurai, U. Quaade, B. Y. Hu, F. P. Murano, and F. Grey, Phys. Rev. Lett. **80**, 2618 (1998).

[8] Y. Nakamura, Y. Mera, and K. Maeda, Appl. Phys. Lett. **77**, 2834 (2000).

[9] Y. Nakamura, Y. Mera, and K. Maeda, Surf. Sci. **487**, 127 (2001).

[10] M. Schlüter and M. Cohen, Phys. Rev. B **17**, 716 (1978).

[11] J. Boland and J. Villarrubia, Phys. Rev. B **41**, 9865 (1990).

[12] Precisely, the 7 × 7 reconstructed structure in $3m$ symmetry is represented by an equivalent sector of $60°$. Practically, however, the experimental distribution of the event frequency was found to be almost symmetric also with respect to $\langle \bar{1}01 \rangle$ axes and, hence, in $6mm$ symmetry.

[13] J. M. Nichols, F. Salvan, and B. Reihl, Phys. Rev. B **34**, 2945 (1986).

[14] H. Öfner, S. L. Surnev, Y. Shapira, and F. P. Netzer, Phys. Rev. B **48**, 10 940 (1993).

[15] Note that the experimentally observed practical symmetry with respect to $\langle \bar{1}01 \rangle$ axes is also reproduced by the present model considering only Γ-K branches.

[16] M. F. Crommie, C. P. Lutz, and D. M. Eigler, Science **262**, 218 (1993).

[17] Y. Hasegawa and Ph. Avouris, Phys. Rev. Lett. **71**, 1071 (1993).

[18] Chr. Wittneven, R. Dombrowski, M. Morgenstern, and R. Wiesendanger, Phys. Rev. Lett. **81**, 5616 (1998).